MOLECULAR AND CELLULAR BIOLOGY, July 2010, p. 3396–3410 Vol. 30, No. 13
0270-7306/10/$12.00 doi:10.1128/MCB.00971-09

Transcriptional Activation of the General Amino Acid Permease Gene *per1* by the Histone Deacetylase Clr6 Is Regulated by Oca2 Kinase▽†¶

Isabelle Kaufmann,[1]‡ Eleanor White,[1] Abul Azad,[1]§ Samuel Marguerat,[2] Jürg Bähler,[2] and Nicholas J. Proudfoot[1]*

Sir William Dunn School of Pathology, University of Oxford, South Parks Road, Oxford OX1 3RE, United Kingdom,[1] and Department of Genetics, Evolution and Environment and UCL Cancer Institute, University College London, London WC1E 6BT, United Kingdom[2]

Received 23 July 2009/Returned for modification 10 September 2009/Accepted 12 March 2010

Expression of nitrogen metabolism genes is regulated by the quality of the nitrogen supply. Here, we describe a mechanism for the transcriptional regulation of the general amino acid permease gene *per1* in *Schizosaccharomyces pombe*. We show that when ammonia is used as the nitrogen source, low levels of *per1* are transcribed and histones in the coding and surrounding regions of *per1* are acetylated. In the presence of proline, *per1* transcription is upregulated and initiates from a more upstream site, generating 5′-extended mRNAs. Concomitantly, histones at *per1* are deacetylated in a Clr6-dependent manner, suggesting a positive role for Clr6 in transcriptional regulation of *per1*. Upstream initiation and histone deactylation of *per1* are constitutive in cells lacking the serine/threonine kinase *oca2*, indicating that Oca2 is a repressor of *per1*. Oca2 interacts with a protein homologous to the *Saccharomyces cerevisiae* transcriptional activator Cha4 and with Ago1. Loss of Cha4 or Ago1 causes aberrant induction of *per1* under noninducing conditions, suggesting that these proteins are also involved in *per1* regulation and hence in nitrogen utilization.

Schizosaccharomyces pombe and *Saccharomyces cerevisiae* are able to use a wide variety of nitrogen sources, although not all support growth equally well. Ammonia is a good nitrogen source, whereas proline is less preferred because it first needs to be metabolized into ammonia. In order to adapt to the quality of the nitrogen supply, yeast initiates new programs of gene expression. Thus, the genes encoding transporters and catabolic enzymes required for proline are repressed when ammonia is available but become derepressed in the presence of proline (46).

In *S. cerevisiae*, proline is taken up by the general amino acid permease Gap1 and by the proline-specific permease Put4. The stability and endocytotic sorting of Gap1 are regulated by Npr1, a protein kinase that acts in the TOR pathway (9). In *Schizosaccharomyces pombe*, the two genes SPAP7G5.06 and SPAC869.10 (now called *per1* and *put4*) encode plasma membrane transporters that are related to *S. cerevisiae* Gap1 and Put4, respectively. In the presence of ammonia, low levels of *per1* and *put4* are transcribed, but their transcription increases when cells are grown in proline (50).

One mechanism by which gene expression can be regulated is through the reversible acetylation of histones. The presence of acetyl groups on histone amino-terminal tails alters chromatin structure, which can affect the recruitment of the transcription machinery to initiation sites, as well as the passage of the elongating polymerase. Histone acetyltransferases (HATs) and histone deactylases (HDACs) function antagonistically in the dynamic acetylation of histones and thus act as regulatory switches of gene activity. Historically, histone acetylation by HATs has been correlated with gene activation, whereas histone deacetylation by HDACs has been associated with gene repression.

Type A HATs modify nucleosomal histones and often act as cofactors for DNA sequence-specific transcription factors, whereas type B HATs acetylate newly synthesized free histones, which is thought to be important for chromatin assembly onto replicating DNA (34). HDACs are usually part of multiprotein complexes and exist as three types, with representatives in both *S. pombe* and *S. cerevisiae*. In *S. pombe*, HDACs are classified as either Clr6- and Hos2-like enzymes (*S. cerevisiae* Rpd3 and Hos2), Clr3-like enzymes (*S. cerevisiae* Hda1), or Sir2-like enzymes (*S. cerevisiae* Sir2). HDACs can act in a targeted way through their recruitment by DNA-binding proteins to promoters, where they locally deacetylate specific histones. They can also act in a nontargeted, global way through deacetylation of larger domains, including coding and surrounding regions (25).

Clr6 exists in two physically and functionally separate complexes. Complex I deacetylates mainly gene promoters, particularly those of highly expressed genes, and represses transcription of the reverse strand of centromeric repeats, which is also driven by bona fide promoter elements (33). In contrast, complex II preferentially targets coding regions to repress spurious sense and antisense transcription of genes, as well as forward-strand transcription of centromeric repeats (33). The *S. cerevisiae* complexes Rpd3L and Rpd3S are structurally and func-

* Corresponding author. Mailing address: Sir William Dunn School of Pathology, University of Oxford, South Parks Road, Oxford OX1 3RE, United Kingdom. Phone: 44 1865 275 566. Fax: 44 1865 275 556. E-mail: nicholas.proudfoot@path.ox.ac.uk.

‡ Present address: Cancer Epidemiology Unit, University of Oxford, Richard Doll Building, Roosevelt Drive, Oxford OX3 7LF, United Kingdom.

§ Present address: Weatherall Institute of Molecular Medicine, John Radcliffe Hospital Headington, Oxford OX3 9DS, United Kingdom.

† Supplemental material for this article may be found at http://mcb.asm.org/.

▽ Published ahead of print on 19 April 2010.

¶ The authors have paid a fee to allow immediate free access to this article.

TABLE 1. Strains used in this study

Strain	Genotype	Reference
A2	*h*$^+$ *ade6-M216 his3-D1 leu1-32 ura4-D18*	Laboratory stock
972	*h*$^-$	Laboratory stock
*oca2*Δ	*h*$^+$ *ade6-M216 his3-D1 leu1-32 ura4-D18 oca2*Δ::*kanMX6*	Laboratory stock
oca2-HA	*h*$^+$ *ade6-M216 his3-D1 leu1-32 ura4-D18 oca2-HA::kanMX6*	Laboratory stock
*oca2*Δ*-20*	*h*$^-$ *oca2*Δ::*kanMX6*	This study
*cha4*Δ	*h*$^+$ *ade6-M216 his3-D1 leu1-32 ura4-D18 cha4*Δ::*kanMX6*	This study
*ago1*Δ	*h*$^+$ *ade6-M216 his3-D1 leu11-32 ura4-D18 ago1*Δ::*kanMX6*	This study
*hat1*Δ	*h*$^+$ *ade6-M216 his3-D1 leu11-32 ura4-D18 hat1*Δ::*kanMX6*	This study
clr6-1	*h*$^-$ *clr6-1*	52
*clr4*Δ	*h*$^+$ *clr4*::*hph*$^+$ *otr1R*(SphI)::*ade6-M210*	Robin Allshire
*oca2*Δ *clr6-1*	*h? ade6-M216 leu1-32 oca2* Δ::*kanMX6 clr6-1*	This study
Wt	*h*$^+$ *leu1-32 ade6-M216 ura4-D18 imr1R*(NcoI)::*ura4*$^+$ *oriI*	Marc Buehler
*rrp6*Δ	*h*$^+$ *leu1-32 ade6-M216 ura4-D18 imr1R*(NcoI)::*ura4*$^+$ *oriI rrp6*Δ::Nat^r	Marc Buehler
Flag-ago1	*h*$^+$ *otr1R*(SphI)::*ura4*$^+$ *ura4-DS/E leu1-32 ade6-M210* Nat^r*-nmt1-3*×FLAG::*ago1*	6

TABLE 2. Genes used in this study

Name	Systematic name
oca2	SPCC1020.10
ppk8	SPAC22G7.08
cha4	SPBC1683.13c
hat1	SPAC139.06
prw1	SPAC29A4.18
per1	SPAP7G5.06
put4	SPAC869.10

tionally related to complexes I and II, respectively. Rpd3L has been implicated in deacetylation of promoter regions, whereas Rpd3S localizes to coding regions and prevents aberrant transcription from cryptic initiation sites (8, 24).

Although HDACs are generally described as transcriptional repressors, several reports have provided evidence that they can also act as activators of gene expression. *S. cerevisiae* Rpd3 has been shown to preferentially associate with the promoters of highly transcribed genes (26). Furthermore, Rpd3 is required for the activation of osmoresponsive, DNA damage-inducible, and anaerobic genes, where upon induction of the gene, Rpd3 is recruited to and deacetylates the promoter (10, 43, 44). Hos2 is required for the transcriptional activation of the *S. cerevisiae GAL* genes, but in this case, it has been shown to deacetylate their coding regions (49). Likewise, *S. pombe* Hos2 promotes high expression of growth-related genes by deacetylating their open reading frames (ORFs) (52).

Here, we describe a mechanism for the transcriptional regulation of the *S. pombe* gene *per1*. We show that upon proline-induced activation, *per1* transcripts with a longer 5′ untranslated region (UTR) are synthesized compared to transcripts produced in the presence of ammonia. Concomitantly, a region spanning the coding and upstream sequences of *per1* is deacetylated in a Clr6-dependent way, suggesting a positive role for Clr6 in transcriptional regulation of the gene. Both 5′-extended transcripts and histone deacetylation are constitutive in cells lacking the serine-threonine kinase Oca2, indicating that Oca2 represses *per1* activation. In the absence of Clr6, Oca2-dependent repression is no longer observed, implying a functional interaction between these two regulators. Oca2 also binds to a protein with homology to the *S. cerevisiae* transcriptional activator Cha4 and to Ago1, a key component of the RNA interference (RNAi) pathway (12). Loss of either protein leads to aberrant regulation of *per1*, suggesting that these proteins are also involved in regulating *per1* expression.

MATERIALS AND METHODS

Strains and media. The *S. pombe* strains used are described in Table 1 (see the supplemental material). All growth conditions, maintenance, and genetic procedures used in this work have been described previously (31). Strains were grown at 30°C in yeast extract (YE) or Edinburgh minimal medium (EMM) with appropriate supplements, 2% glucose, and either 0.5% ammonia or 10 mM proline as a nitrogen source. Rapamycin was dissolved in dimethyl sulfoxide (DMSO)/methanol and added at 0.3 μM.

Genetic manipulations. The *cha4*Δ, *ago1*Δ, and *hat1*Δ genes (Table 2) were disrupted in strain A2 via homologous recombination using a PCR fragment amplified from the plasmid pFa6a-KanMX6 (3) and the primers listed in Table 3 (see the supplemental material). Gene replacement was confirmed by PCR using primers specific for *KanMX6* and gene-specific sequences. For generation of the double mutants *oca2*Δ *clr6-1* and *oca2*Δ *hat1*Δ, the haploid strains *oca2*Δ and *clr6-1*, and *oca2*Δ*-20* and *hat1*Δ, respectively, were crossed on Sporulation plates and incubated at 25°C for 3 days. Tetrads were dissected using a Singer Instruments MSM system, and spores were tested by colony PCR for the presence of the disrupted *oca2*Δ::*KanMX6* and *hat1*Δ::*KanMX6* alleles and by DNA sequencing for the *clr6-1* mutation.

RNA analysis. Total RNA was isolated from exponentially growing *S. pombe* cells (~1×10^7 cells/ml) using the hot-phenol method as previously described (27). For whole-genome expression profile analysis, 10 to 20 μg of total RNA was labeled by direct incorporation of either fluorescent Cy3- or Cy5-dCTP (GE Healthcare), and the fluorescently labeled products were hybridized to *S. pombe* cDNA microarrays as previously described (27). The microarrays were scanned using a GenePix 4000B laser scanner (Axon Instruments), and fluorescence intensity ratios were calculated with GenePix Pro (Axon Instruments). The data were normalized using Perl script as previously described (27). For quantitative reverse transcription (qRT)-PCR, 200 ng of total RNA was reverse transcribed with Superscript III Reverse Transcriptase (Stratagene), followed by qPCR with a QuantiTect SYBR green kit (Qiagen) on a Corbett Rotor-Gene 3000 machine using the primers listed in Table 3. Values were normalized to actin and expressed as percentages of wild-type (wt) values. For Northern blot analysis, 15 μg of total RNA was separated on 1% formaldehyde agarose gels. Templates for single-stranded RNA probes were amplified from *S. pombe* genomic DNA using the primers listed in Table 3. The probes were *in vitro* transcribed using T3 or T7 RNA polymerase (T7/T3 MAXI kit; Ambion) for detection of sense or antisense transcripts, respectively, and hybridized at 62°C (7).

***S. pombe* whole-cell protein extracts.** Cells were grown to ~1×10^7 cells/ml, harvested, washed in water, and resuspended in lysis buffer (50 mM Tris-HCl, pH 7.5, 150 mM NaCl, 5 mM $MgCl_2$, 0.05% NP-40, 10% glycerol, 1 mM dithiothreitol [DTT], 1 mM phenylmethylsulfonyl fluoride [PMSF], and protease inhibitor cocktail [Roche]). The cells were disrupted with glass beads by vortexing them 12 times for 30 s each time at 4°C, followed by centrifugation. The protein concentration was determined by measuring absorbance at 280 nm. SDS-PAGE and Western blot analysis were performed according to standard procedures using antihemagglutinin (anti-HA) (F-7; Santa Cruz) and antitubulin (kindly provided by K. Gull) antibodies.

Recombinant and *in vitro*-translated proteins. For expression of GST-Oca2 in *Escherichia coli*, the whole *oca2* ORF was PCR amplified from *S. pombe* genomic DNA using primers P14 and P15 (Table 3) and cloned into pGEX4T1 (Pharmacia), giving rise to pGEX4T1-Oca2. For *in vitro* translation of *ago1*, the *ago1* ORF was subcloned from clone pDONR210 (kindly provided by R. Allshire) into pBS using oligonucleotides Ago1F/Ago1R. For *in vitro* translation of *cha4* and *prw1*, the respective ORFs were PCR amplified from *S. pombe* cDNA using oligonucleotides Cha4FT7/Cha4R or Prw1FT7/Prw1R. For *in vitro* translation of *hat1* and *mis16*, the respective ORFs were PCR amplified from *S. pombe* cDNA using oligonucleotides Hat1F/Hat1R and Mis16F/Mis16R and cloned into pBS. *In vitro* translation was performed using a TNT-coupled transcription and translation rabbit reticulocyte lysate (Promega) and [^{35}S]methionine. GST-Oca2 was expressed in BL21-CodonPlus-RP cells (Stratagene) and purified according to standard procedures with GSH-Sepharoase (Pharmacia). Proteins were concentrated in Centri-

TABLE 3. Primers used in this study

Name	Sequence or reference	Purpose
1F	TGTGTCTCGGCTTACCCTTC	ChIP *per1*
1R	GCGGAAAGAGACGGATAACA	ChIP *per1*; 5′ RACE
1BR	GTGCAATCTACTAGCAACCAAG	5′ RACE
2F	GCTCTCCAAGTGCCAGTTTC	ChIP *per1*
2R	GCCGCACAATATGGATAAGG	ChIP *per1*
3F	CGCATCTTGCATTATTTCACC	ChIP *per1*
3R	AAACGATTGGGAAACACTCG	ChIP *per1*; 5′ RACE
4F	GTCGCCAGATCGCTCTATTG	ChIP *per1*
4R	TGGGATGAATGTCGAAAACA	ChIP *per1*; 5′ RACE
5F	GCGGTGGTGTTCCTACTGAT	ChIP; qRT-PCR
5R	GCACGAGGGAGAGACTTTTG	ChIP; qRT-PCR
6F	TGATTTAGACACGGGACTTCG	ChIP *per1*
6R	CAAAGAGATTGCCAAATCCA	ChIP *per1*
7F	CGTTGTAAGTTTATATGTTGAAGCA	ChIP *per1*
7R	TGCGAATGCAAGGCATAATA	ChIP *per1*
8F	ATATAATGTTGAGCTCCTTGGTTAGC	ChIP *per1*
8R	TGAGCTTGATAAGGCGGTCT	ChIP *per1*
Put4BF	AAAAAGGCGTTGCAGTATGA	ChIP *put4*
Put4BR	TTTCTCCGTACTTCTTTTCAACG	ChIP *put4*
Adh1PF	CTTCCGCGTCTCATTGGT	ChIP *adh1*
Adh1PR	TTGCTTAAAGAAAAGCGAAGG	ChIP *adh1*
dhF	21	ChIP *dh*
dhR	21	ChIP *dh*
Put4F	ACATGATCGCTTGGGTTTTC	qRT-PCR *put4*
Put4R	TTAGGGATGTTACGCCTTGG	qRT-PCR *put4*
Adh1F	CGTATTGACTCTATCGAGGCTCTT	qRT-PCR *adh1*
Adh1R	CTTGGAAAGGTCCAAGACGA	qRT-PCR *adh1*
RT-PCR1	51	RT-PCR *dh*
RT-PCR2	51	RT-PCR *dh*
ACTF	51	RT-PCR *act1*
ACTR	51	RT-PCR *act1*
ORFT7	TAATACGACTCACTATAGGGAGAGCGGTGGTGTTCCTACTGAT	Northern *per1*
ORFT3	AATTAACCCTCACTAAAGGGAGACCAACACGAAGGGAGAGGTA	Northern *per1*
US2T7	TAATACGACTCACTATAGGGAGAGCCCATTCCCATTCAATTTT	Northern *per1*
US2T3	AATTAACCCTCACTAAAGGGAGAATGTTTGAGCGCGTGTATGT	Northern *per1*
US1T7	TAATACGACTCACTATAGGGAGACTGCTGCAAAACTTTGGTTG	Northern *per1*
US1T3	AATTAACCCTCACTAAAGGGAGATTAGTTACCCTATTTGGAAG	Northern *per1*
RplAT7	TAATACGACTCACTATAGGGAGAGCTCGTATCTGTGCCAACAA	Northern *rpl1002*
RplAT3	AATTAACCCTCACTAAAGGGAGAGTAGCAACCGTCGGGAATAA	Northern *rpl1002*
RplBT7	TAATACGACTCACTATAGGGAGATGGTGTTGGATGAATCGGTA	Northern *rpl1002*
RplBT3	AATTAACCCTCACTAAAGGGAGACGTGGAAGTAGATGCGGAGT	Northern *rpl1002*
Adh1T7	TAATACGACTCACTATAGGGAGATTCAAGGTGACTGGCCTCTT	Northern *rpl1002*
Adh1T3	AATTAACCCTCACTAAAGGGAGACAAGGCACGATAGCAAGTGA	Northern *adh1*
Prw1FT7	GTGATAACTACTAATACGACTCACTATAGGGAGAATGGC TGTATCAGCTGTTC	Northern *adh1*
Prw1R	TTAACTTAAATATGCCGTAG	*In vitro* translation
Cha4FT7	GTGATAACTACTAATACGACTCACTATAGGGAGAATGCAAATGAAACCCCGAC	*In vitro* translation
Cha4R	TTAATATTTTACATTGGGAG	*In vitro* translation
		In vitro translation
Hat1F	ATGAGTGCTG TTGATGAATG	pBS-*hat1*
Hat1R	TTAGGAAGAAGATTGAGCAAG	pBS-*hat1*
Mis16F	ATGTCAGAGGAAGTAGTCC	pBS-*mis16*
Mis16R	TTACTCCAGATCCCTAGGAG	pBS-*mis16*
Ago1F	GATGTCGTATAAACCAAGCTCAG	pBS-*ago1*
Ago1R	TTACATATACCACATCTTTGTTTTC	pBS-*ago1*
P14	ACCCCCGGGCATGTCTGTCACCCT	pGEX4T1-*oca2*
P15	GGACCCGGGATGCTTTGCAGGTGG	pGEX4T1-*oca2*
Hat1KanF	GAGCTAGAAATCTATATAATAGTAAATATTTTTTAATAATAACAGGTGTAGCACGTGAAAGCGGATCCCC GGGTTAATTAA	*hat1*Δ
Hat1KanR	TAAATTTTGGAAAAAGCAGTTCATTATGAGGAATTGTTTGAATTTTTATAAGGTGCCTTTGAATTCGAGC TCGTTTAAAC	*hat1*Δ

con MWCO-10 (Millipore) and dialyzed against buffer D (50 mM Tris-HCl, pH 7.9, 50 mM KCl, 10% glycerol, 0.02% NP-40, 0.1 mM DTT) for 4 h at 4°C.

In vitro protein binding assays. Purified glutathione *S*-transferase (GST) protein (1 μg) was incubated with 5 to 6 μl of *in vitro*-translated protein for 1 h at 25°C in binding buffer (50 mM Tris-HCl, pH 7.9, 75 mM KCl, 10% glycerol, 0.01% NP-40, 0.05 mg/ml bovine serum albumin [BSA]). Protein complexes were bound to GSH-Sepharose that was preblocked with BSA, washed four times with IPP150 (10 mM Tris-HCl, pH 7.9, 150 mM KCl, 0.1% NP-40), eluted with SDS loading buffer, and analyzed by SDS-PAGE and autoradiography.

ChIP analysis. Chromatin immunoprecipitation (ChIP) analysis was performed using exponentially growing cells ($\sim 1 \times 10^7$ cells/ml) as described previously (35), except that the cells were broken using a MagNA Lyser (Roche). Chromatin was shared by sonication for 30 s on/30 s off at medium setting for 10 min. Cross-linked proteins were immunoprecipitated using antibody H8 (ab5408; Abcam) or anti-H4K12ac (ab1761; Abcam). Immunoprecipitated DNA was quantified using real-time PCR with a QuantiTect SYBR green kit (Qiagen) on a Corbett Rotor-Gene 3000 machine. The primer efficiency was normalized using genomic DNA. ChIP signal values were expressed as percentages of input DNA corrected for the no-antibody background. The sequences of primers used for amplification of precipitated DNA are listed in Table 3.

RESULTS

Oca2 is involved in the utilization of different nitrogen sources. A previous genetic screen aimed at identifying multicopy suppressors of a transcription termination mutant in *S. pombe* led to the isolation of *oca2*, a predicted serine/threonine kinase (2; A. Azad and N. J. Proudfoot, unpublished data). *oca2* was independently identified in a screen for *S. pombe* genes causing

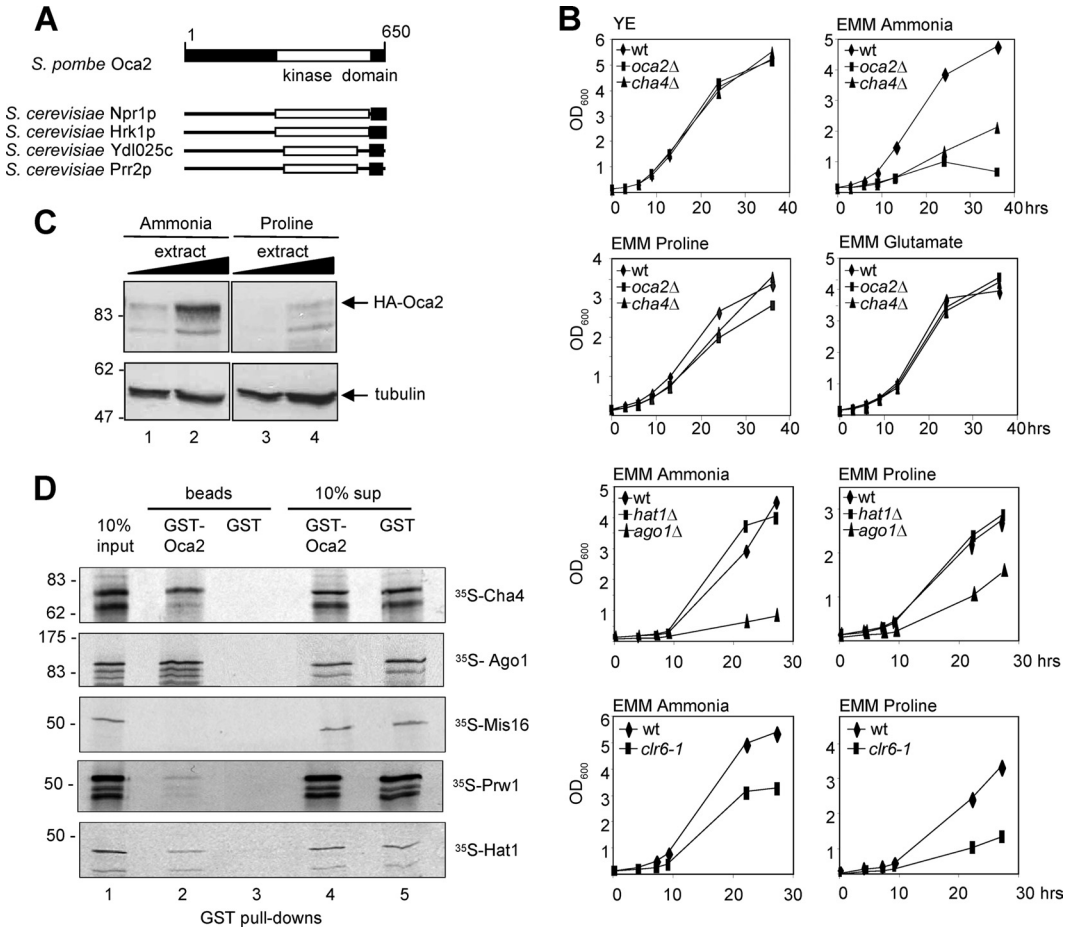

FIG. 1. (A) Oca2 is related to *S. cerevisiae* Npr1. Shown is a schematic representation of Oca2 protein and Oca2-related proteins based on amino acid sequence homology. The C-terminal kinase domain is denoted by a white box. Regions with sequence similarity are indicated. (B) *oca2*Δ cells grow slowly in EMM containing ammonia. The wt and mutant cells indicated were grown to mid-exponential phase in YE and diluted in EMM containing ammonia, proline, or glutamate, and the optical density at 600 nm (OD_{600}) was measured at the indicated time points. (C) Oca2 protein decreases when cells are grown in proline. Total protein extract from an *HA-oca2*-tagged strain grown in ammonia or proline and 150 and 300 μg of total protein extract were analyzed by Western blotting using antibodies against HA (top) and tubulin (bottom). (D) Oca2 interacts with Cha4, Ago1, Prw1, and Hat1. GST pulldown experiments employed recombinant GST-Oca2 or GST and *in vitro*-translated Cha4, Ago1, Mis16, Prw1, and Hat1. Bound proteins were analyzed by SDS-PAGE and autoradiography. Lane 1, 10% of the total input of each *in vitro*-translated protein; lanes 2 and 3, bound proteins; lanes 4 and 5, 10% of the supernatant of each binding reaction after removal of the GSH beads. The calculated molecular masses were as follows: Cha4, 72 kDa; Ago1, 94 kDa; Mis16, 48 kDa; Prw1, 48 kDa; Hat1, 44 kDa. The lower-molecular-mass bands correspond to degradation or premature termination products of the *in vitro* translation reaction.

overexpression-mediated cell cycle arrest and cell elongation (45). Oca2-His_6 expressed in Sf9 insect cells phosphorylates myelin basic protein (MBP) *in vitro*, confirming that Oca2 has kinase activity (see Fig. S1A in the supplemental material). Moreover, we found that Oca2 preferentially phosphorylates serines and threonines surrounded by basic residues (see Fig. S1B in the supplemental material). Proteomic analysis revealed that Oca2 belongs to a family of fungus-specific protein kinases that regulate plasma membrane transporters (20). In *S. cerevisiae*, the closest homologs of Oca2 are Npr1, Hrk1, Ydl025c, and Prr2, with the homology mainly in the C-terminal kinase domain (Fig. 1A). In *S. pombe*, a second Oca2-like protein kinase (SPAC22G7.08) with unknown function exists (5).

S. cerevisiae Npr1 regulates nitrogen utilization by controlling the stability and sorting of the general amino acid permease Gap1 in response to nitrogen (9). Interestingly, we found that the loss of *oca2* leads to a slow-growth phenotype when cells are grown in minimal medium (EMM) with ammonia as the nitrogen source, but cells grow normally in proline or glutamate (Fig. 1B), suggesting that Oca2 has a role in the response to nitrogen availability similar to that of Npr1. In addition, *oca2*Δ cells are resistant to rapamycin in minimal medium with ammonia (even though growth is already slow), another similarity to *S. cerevisiae* Npr1 (40) (see Fig. S2A in the supplemental material). Using an *HA-oca2*-tagged strain and Western blot analysis of whole-cell extracts, we also observed that the levels of Oca2 protein were higher in cells grown in ammonia than in cells grown in proline (Fig. 1C), suggesting that Oca2 is required for growth in ammonia but is dispensable when proline is used. The observed molecular mass of HA-Oca2 was slightly larger than predicted (74.5 kDa). This difference could be due to phosphorylation, as phosphatase treat-

ment of HA-Oca2 leads to a decrease in molecular mass (see Fig. S1C in the supplemental material).

To further characterize Oca2, we performed a yeast two-hybrid screen to identify Oca2-interacting proteins. Using Oca2 fused to the *GAL4* DNA-binding domain as bait, we isolated two positive clones, SPBC1683.13c and *ago1* (A. Azad, data not shown). SPBC1683.13c contains a Zn_2-C_6 zinc finger domain and is related to the *S. cerevisiae* transcriptional activators Cha4 and Tea1, which regulate serine-regulated and Ty1 enhancer-regulated genes, respectively (10a, 17). Because of its greater homology to *S. cerevisiae* Cha4, we renamed SPBC1683.13c Cha4. Ago1 is a subunit of the RNA-induced transcriptional silencing (RITS) complex involved in RNAi-induced heterochromatin formation (12).

To confirm the interactions obtained by the two-hybrid screen, we performed GST pulldown experiments using recombinant GST-tagged Oca2 and *in vitro*-translated Cha4 and Ago1, respectively. Bound proteins were analyzed by SDS-PAGE and visualized by autoradiography. As shown in Fig. 1D, about 10% of the total input Cha4 and Ago1 were bound by GST-Oca2, but not by GST, confirming that Oca2 interacts with the proteins.

S. cerevisiae Npr1 has been shown to bind to Cac3 (Msi1), a subunit of the chromatin assembly factor CAF1 and the negative regulator of the RAS/cyclic AMP (cAMP) pathway (22). The *S. pombe* genome encodes three proteins with sequence homology to Cac3: Mis16, a kinetochore protein (15); Prw1, a subunit of the Clr6 HDAC complex (33); and Hat1, a type B HAT (4). To test whether the interaction between Npr1 and Cac3 was conserved in *S. pombe*, we performed GST pulldown experiments using *in vitro*-translated Mis16, Prw1, or Hat1. As shown in Fig. 1D, Oca2 bound to Hat1 and weakly to Prw1, but not to Mis16. These associations appear weaker than those of Oca2 with Cha4 and Ago1. It is possible that the interactions between Oca2 and Prw1 or Hat1 are relatively transient and thus unstable, as was found for *S. cerevisiae* Nrp1 and Cac3 (22).

Because of the observed interaction of Oca2 with Cha4, Ago1, Prw1, and Hat1, we also measured the growth phenotypes of strains carrying mutations in these genes (Fig. 1B). *cha4*Δ cells had a phenotype similar to that of *oca2*Δ cells, with slow growth in EMM containing ammonia as the nitrogen source but normal growth in proline. Likewise, cells lacking Ago1 showed a moderately slow growth phenotype in proline but a severe growth defect in ammonia. Prw1 is a subunit of the Clr6-containing HDAC; we therefore looked at the growth phenotype of a strain carrying the *clr6-1* mutant allele (11). *clr6-1* mutant cells grew slightly more slowly in ammonia, but their growth was severely impaired in proline, thus showing growth characteristics opposite to those of *oca2*Δ, *cha4*Δ, and *ago1*Δ. Finally, *hat1*Δ cells grew normally in both ammonia and proline. As with *oca2*Δ, *cha4*Δ and *ago1*Δ are resistant to rapamycin (see Fig. S2A in the supplemental material).

Membrane transporter genes are upregulated in the absence of Oca2. To assess the role of Oca2 in gene expression, we carried out a whole-genome expression analysis of *oca2*Δ cells grown in minimal medium with ammonia as the nitrogen source. Compared to a wt strain, cells lacking *oca2* showed downregulated (≥1.5-fold) expression of 36 genes, many of which code for proteins of unknown function (data not shown). The expression of six genes was increased ≥1.5-fold (Fig. 2A), among them *per1*. Thirty-four genes, many of which code for membrane transporter proteins, including *put4*, showed more modest (≥1.25-fold) upregulation in *oca2*Δ cells. We also noticed that a large number of the upregulated genes were clustered near either subtelomeric regions or the centromere. Thus, of the 21 genes that were upregulated ≥1.25-fold on chromosome 1, for example, 11 were located within 150 kb of the telomeric ends, including the first (SPAC212.11; *tlh1*) and the last (SPAC750.07c) ORFs at the left and right telomeric ends, respectively, and one (*per1*) was the RNA polymerase II (Pol II) transcribed gene closest to the left outermost region of the centromere (see Fig. 6A).

To validate the data from the above expression-profiling analysis, we determined the mRNA expression levels of selected genes using qRT-PCR. We analyzed the genes *per1* and *put4*, whose transcription is regulated by proline (50) and whose aberrant expression in *oca2*Δ cells could thus be linked to the growth phenotype we observed in that strain. We found that in an *oca2*Δ strain grown in EMM with ammonia, the levels of *per1* and *put4* transcripts were upregulated between 2- and 3-fold compared to a wt strain, confirming the expression-profiling analysis (Fig. 2B). Note that these transcript level increases are greater than those observed in the genome-wide expression analysis, reflecting the greater dynamic range of qRT-PCR analysis. A similar or slightly greater increase of *per1* and *put4* expression was detected in wt cells grown in proline, consistent with earlier reports (50). In contrast, levels of *adh1* mRNA remained constant in *oca2*Δ cells or in wt cells grown in either nitrogen source. Overall, we showed that the absence of Oca2 leads to increased levels of *per1* and *put4* transcripts, similar to wt cells that are grown in proline. This suggests that in the presence of ammonia, Oca2 acts as a repressor of these genes.

5′-extended transcripts accumulate upon activation of *per1*. To characterize the expression profile of *per1* in more detail, we performed a Northern blot analysis with total RNA isolated from wt and *oca2*Δ strains and strand-specific probes for *per1*. Using a probe for the ORF of *per1* (probe ORF), we detected one major transcript in RNA from wt cells grown in ammonia (transcript A) (Fig. 3A, lane 1). Compared to the known size of the actin mRNA, the size of transcript A was estimated to be around 2,800 bp, which is about 1,000 bp larger than the ORF of *per1*. A slightly shorter transcript was also observed (transcript A′). When wt cells were grown in proline, an additional major transcript of about 3,800 bp was detected (transcript B) (Fig. 3A, lane 2), whereas transcript A′ was no longer observed. Both, transcripts A and B were constitutively expressed in *oca2*Δ cells irrespective of the nitrogen source (lanes 3 and 4). Using a probe mapping to a region 600 bp downstream of the *per1* stop codon, transcripts A and B were no longer detectable (data not shown), whereas a probe specific for a region 1,000 bp upstream of the start codon (probe US2) (Fig. 3A, middle) detected both mRNAs. Using a probe that hybridized even further upstream (probe US1) (Fig. 3A, right), we detected transcript B, but not transcript A, indicating that transcript B is a 5′-extended form of transcript A. Probe US1 also detected several additional, shorter transcripts (transcript C) (lanes 14 to 18). To rule out the possibility that transcript B was due to transcriptional read-through from the upstream ribosomal protein gene *rpl1002* into *per1* (see Fig. S3 in the

A

Systematic name	name	-fold up	function	*S.cerevisiae* homolog
SPAC11D3.18c	*tna1*	1.7	nicotinic acid plasma membrane transporter (predicted)	*TNA1*
SPAC11D3.14c		1.7	oxoprolinase (predicted)	
SPAC11D3.15		1.6	oxoprolinase (predicted)	
SPAC750.07c		1.6	Protein of unknown function	
SPBC530.02		1.5	membrane transporter	
SPAP7G5.06	*per1*	1.5	General amino acid permease (predicted)	*GAP1*
SPAC5H10.01		1.5	Protein of unknown function	
SPAC1F7.07c	*fip1*	1.5	iron permease	
SPBC1683.12		1.4	nicotinic acid plasma membrane transporter (predicted)	
SPCC24B10.22	*mip1*	1.4	DNA polymerase gamma catalytic subunit	
SPAC212.11	*tlh1*	1.4	RecQ type DNA helicase	
SPAC1F8.03c	*str3*	1.4	siderochrome-iron transporter	*ARN1*
SPCPB1C11.01	*amt1*	1.4	ammonium transporter (predicted)	*MEP1*
SPBC36.03c		1.4	membrane transporter	*TPO1*
SPBC1683.09c	*frp1*	1.4	ferric-chelate reductase	*FRE1*
SPAC212.08c		1.4	Protein of unknown function	
SPAC1B3.16c	*vht1*	1.4	vitamin H transporter	*VTH1*
SPBP4G3.02	*pho1*	1.3	acid phosphatase	*PHO1*
SPBC27.04		1.3	Protein of unknown function	
SPAC1399.02		1.3	membrane transporter	*AZR1*
SPAC644.06c	*cdr1*	1.3	serine/threonine protein kinase	*KCC4*
SPBC27.05		1.3	Protein of unknown function	
SPAPB18E9.02c	*ppk18*	1.3	serine/threonine protein kinase (predicted)	*RIM15*
SPBC1105.05	*exg1*	1.3	glucan 1, 3-beta-glucosidase I/II precursor	*EXG1*
SPBC3E7.06c		1.3	membrane transporter	
SPBC8E4.01c		1.3	inorganic phosphate transporter (predicted)	*PHO84*
SPAC869.10c	*put4*	1.3	amino acid transporter (predicted)	*PUT4*
SPBC17D1.01		1.3	sequence orphan	*SPP41*
SPAC22A12.06c		1.3	Protein of unknown function	
SPAC5H10.06c	*adh4*	1.3	alcohol dehydrogenase	*ADH4*
SPAC11D3.17		1.3	zinc finger protein	
SPBC26H8.11c		1.3	Protein of unknown function	
SPAC4A8.04	*isp6*	1.3	serine protease	*PRB1*
SPCC1281.06c		1.3	acyl-coA desaturase (predicted)	*OLE1*
SPCC1906.02c		1.2	CUE domain protein	

B

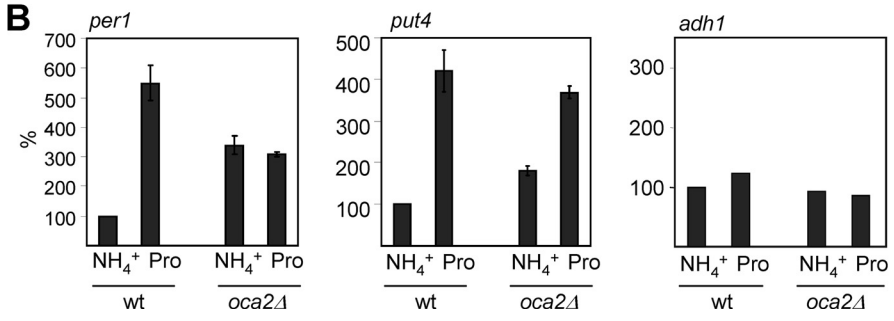

FIG. 2. Loss of *oca2* leads to upregulation of genes coding for membrane transporters. (A) Whole-genome expression analysis of *oca2*Δ cells grown in EMM with ammonia. Genes that were upregulated ≥1.25-fold are listed. (B) *oca2*Δ cells show increased mRNA levels of *per1* and *put4*. mRNA levels were determined by quantitative RT-PCR, normalized to actin, and expressed as percentages of wt cells grown in ammonia. The data shown represent the average and standard error of the mean (SEM) of at least three independent experiments. Controls without reverse transcriptase gave background signals (not shown).

supplemental material), we also tested probes mapping to the ORF (probe A) or immediately downstream of *rpl1002* (probe B). Probe A detected a transcript of about 700 bp, corresponding to the size of *rpl1002*, while probe B detected low levels of short 3′-extended transcripts, particularly for wt cells grown in ammonia. No longer read-through transcripts the same size as transcript B were detected. Overall, these data suggest that in wt cells, proline-dependent stimulation leads to the production of a longer *per1* mRNA derived from an upstream initiation site. Furthermore, in *oca2*Δ cells, this profile of *per1* expression is constitutive.

We also examined the expression pattern of *per1* in *cha4*Δ cells. In RNA from *cha4*Δ cells grown in ammonia, we detected transcripts A, B, and C, similar to *oca2*Δ (Fig. 3A, lanes 5, 11, and 17). However, *cha4*Δ cells grown in proline produced transcript A but only small amounts of transcripts B and C, a profile more similar to that of wt cells grown in ammonia. Therefore, *cha4* cells showed aberrant expression of *per1* in

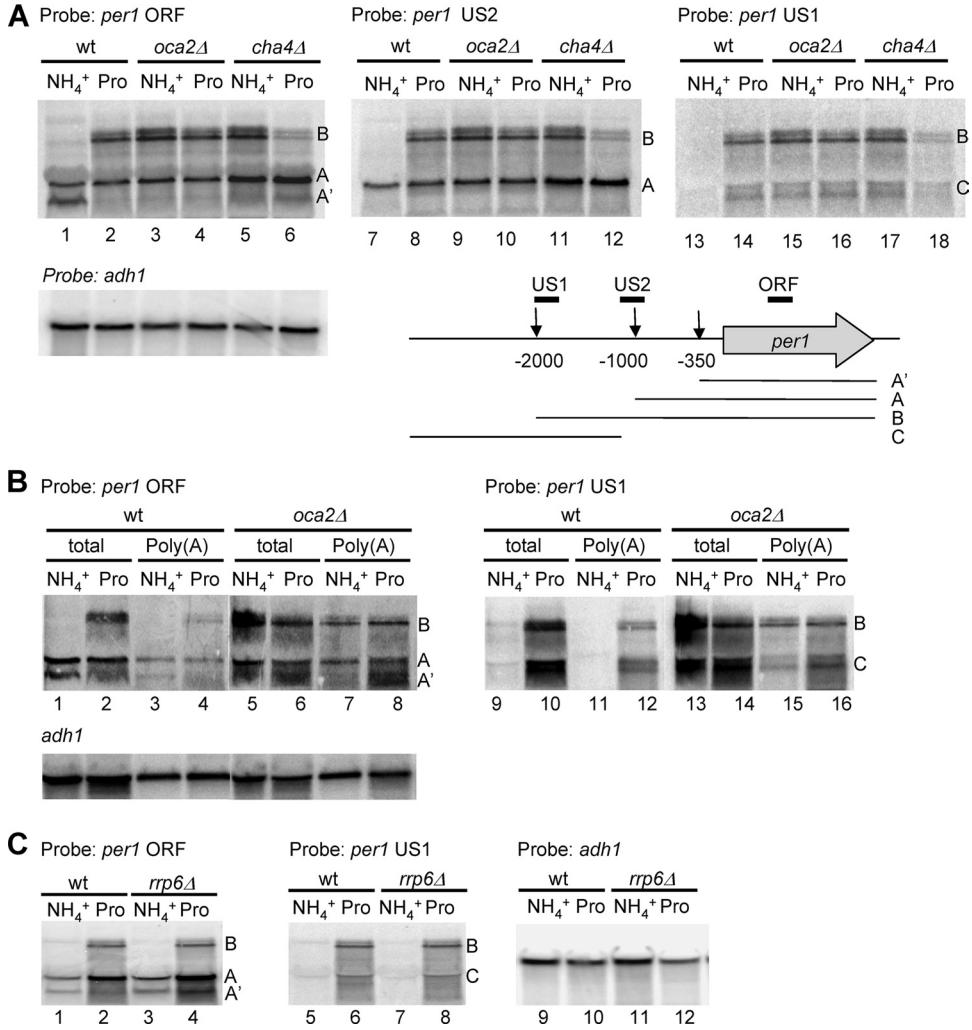

FIG. 3. 5′-extended *per1* transcripts. (A) Northern blot analysis of total RNA isolated from wild-type, *oca2*Δ, and *cha4*Δ cells grown in either ammonia or proline. The Northern blot was consecutively probed with single-stranded RNA probes mapping to the ORF (left), a region 1 kb upstream of the AUG (US2; middle), or a region 1.7 kb upstream of the AUG (US1; right) to detect *per1* sense transcripts. A probe specific for the ORF of *adh1* was used as a loading control. A summary of the transcripts detected by Northern blotting with their average transcription initiation site as determined by 5′ RACE is shown schematically. (B) 5′-Extended transcripts of *per1* are polyadenylated. Total RNA and poly(A)-selected RNA were analyzed by Northern blotting as indicated. The blot was subsequently probed for *adh1* as a loading control. (C) Northern blot of total RNA isolated from wt and *rrp6*Δ cells using probes ORF (left), US1 (middle), and *adh1* (right).

both nitrogen sources, whereas *oca2*Δ cells showed a defect only in ammonia.

Rapamycin has been shown to reduce the expression of *per1* and *put4* (50). Adding rapamycin to *oca2*Δ or *cha4*Δ cells that were grown with ammonia led to a reduction of transcripts B and C and to an increase of transcript A, a profile closer to the one displayed by wt cells grown with this nitrogen source (see Fig. S2B in the supplemental material). This observation could thus explain the improved growth phenotype of *oca2*Δ and *cha4*Δ in the presence of the drug.

To further characterize the different *per1* transcripts, we performed a rapid amplification of cDNA ends (RACE) analysis to map their transcription initiation sites. Using RNA isolated from wt and *oca2*Δ cells grown with either ammonia or proline, three main populations of 5′-RACE products were obtained, corresponding to transcription initiation sites around bp −350, −1000, and −2000, respectively (Fig. 3A; see Fig. S4 in the supplemental material). The product relating to a 5′ end at bp −2000 was obtained only with RNA from wt cells grown in proline or *oca2*Δ cells grown with ammonia or proline, confirming the results from Northern blot analysis.

To investigate whether the *per1* transcripts were polyadenylated, we performed Northern blot analysis on poly(A)-selected RNA using probes US1 and ORF (Fig. 3B). Transcripts A, A′, B, and C were all polyadenylated, a hallmark of protein-encoding transcripts, but also of unstable regulatory transcripts degraded by the exosome (39). To test whether transcripts B and C were cryptic transcripts that were degraded in the nucleus, we analyzed RNA isolated from an *rrp6*Δ mutant strain that is defective in the nuclear exosome function. As shown in Fig. 3C, lack of *rrp6* did not lead to the stabilization and

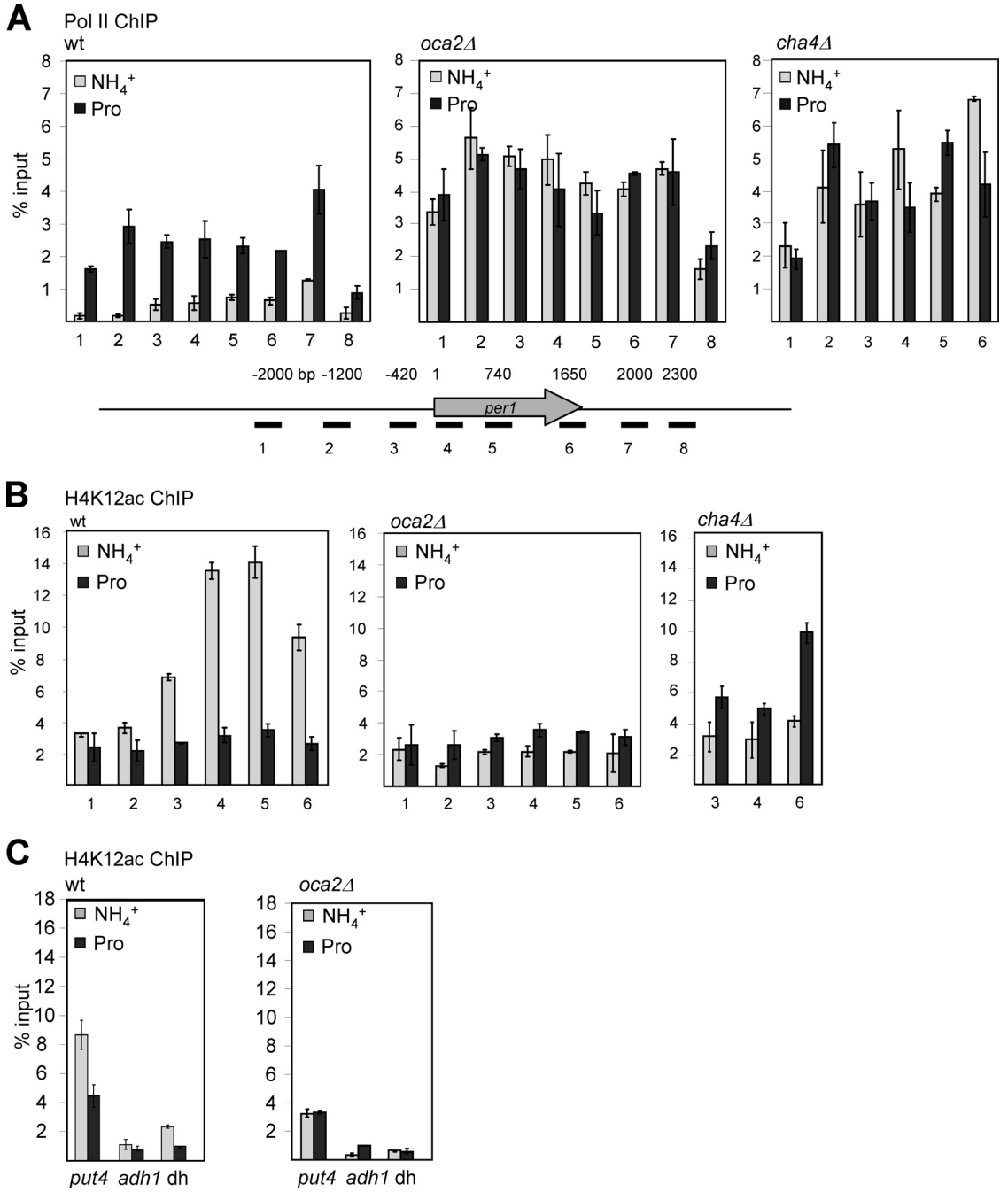

FIG. 4. The binding of Pol II increases and H4K12 acetylation decreases upon transcriptional activation of *per1*. (A) Pol II ChIP of wt, *oca2*Δ, and *cha4*Δ cells grown in EMM containing either ammonia or proline (Pro). Pol II was precipitated using an antibody against the CTD of Pol II (H8). The positions of the PCR primers across *per1* are indicated. ChIP signal values are expressed as percentages of input DNA corrected for the no-antibody control. The data shown represent the average and SEM of at least three independent experiments. (B) H4K12ac ChIP of wt, *oca2*Δ, and *cha4*Δ cells using anti-H4K12ac antibody. Primer pairs and quantification are the same as in panel A. (C) H4K12ac ChIP of wt and *oca2*Δ cells using primer pairs specific for the ORFs of *put4* and *adh1* and the centromeric-repeat dh.

accumulation of transcripts B and C, indicating that they are not cryptic unstable transcripts.

Pol II occupancy and histone acetylation of *per1* increases upon transcriptional stimulation. The Pol II distribution at *per1* was assessed using ChIP analysis. Wt cells grown in ammonia showed a low level of Pol II-associated chromatin starting between 1 and 0.5 kb upstream of the translation start codon and decreasing at about 500 bp beyond the stop codon (Fig. 4A, left). In contrast, Pol II levels at chromatin isolated from wt cells grown in proline were increased 3- to 5-fold. Significantly, Pol II was also detectable 2 kb upstream of the AUG (probes 1 and 2).

The Pol II profile for chromatin from *oca2*Δ cells grown in ammonia was similar to that of wt cells grown in proline, with high levels of binding over the *per1* coding and upstream regions (Fig. 4A, middle). *oca2*Δ cells grown in proline showed similar high levels of Pol II binding, particularly in the region 2 kb upstream of the AUG (probe 1). These results are consistent with the Northern blot data (Fig. 3A). In particular, the *per1* 5′-extended transcript B appears to correlate with the higher Pol II ChIP signals. Chromatin from *cha4*Δ cells grown in either ammonia or proline gave a Pol II profile similar to that of *oca2*Δ cells, except that Pol II levels over probe 1 were lower (Fig. 4A, right). Overall, the results from these ChIP analyses suggest that the changes in the *per1* mRNA profile reflect altered Pol II distribution and transcription.

A likely explanation for how Pol II transcription of *per1* is regulated is through changes of the chromatin structure. Oca2 interacts with Prw1, a subunit of the Clr6 HDAC, and with the histone acetyltranferase Hat1 (see Fig. 1D). Clr6 deacetylates several lysines in histones 3 and 4, including H4K12, and this residue is also a main substrate for Hat1 (34, 38). Using ChIP analysis, we found that the level of H4K12 acetylation was increased when wt cells were grown in ammonia compared to growth in proline (Fig. 4B, left). A region starting 2 kb upstream of the translation start site and spanning the ORF showed 1.5- to 4-fold-higher levels of H4K12 acetylation in the presence of ammonia than in the presence of proline, with the difference being most pronounced over the ORF. In contrast, H4K12 acetylation was low in the *oca2*Δ strain for both nitrogen sources (Fig. 4B, middle). The levels of histone H3 at *per1* did not change significantly between the two growth conditions and strains, indicating that the difference in H4K12 acetylation was not caused by a change in overall histone levels (see Fig. S5 in the supplemental material). Thus, at *per1*, increased acetylation of H4K12 correlates with transcriptional repression of the upstream transcript.

We also looked at the profile of H4K12 acetylation in *cha4*Δ cells (Fig. 4B, right). In the presence of ammonia, levels of H4K12 acetylation over the *per1* ORF were lower than the in wt strain, similar to the *oca2*Δ strain. However, when *cha4*Δ cells were grown in proline, they exhibited an increase of H4K12 acetylation compared to wt and *oca2*Δ cells. Overall, these results demonstrate that in wt cells, transcriptional activation of *per1* in response to proline correlates with deacetylation of H4K12 and with the appearance of longer, 5′-extended transcripts. In the *oca2*Δ strain, these effects were constitutive irrespective of the nitrogen source. *cha4*Δ cells showed deacetylation and activation of *per1* under repressing conditions, similar to *oca2*Δ cells, but failed to do so under derepressing conditions.

H4K12 acetylation was also analyzed at the *put4* gene (Fig. 4C). H4K12 acetylation at *put4* was increased in wt cells using ammonia compared to proline (Fig. 4C, left). Again, *oca2*Δ cells gave similar lower levels of H4K12 acetylation at this locus in both nitrogen sources (Fig. 4C, right). In both strains, H4K12 acetylation at the *adh1* locus did not change significantly, indicating that the effects seen at *per1* and *put4* are gene specific. Furthermore, H4K12 acetylation at the centromeric repeat was slightly higher in wt cells grown in ammonia than in those grown in proline, whereas they were the same in *oca2*Δ cells for both nitrogen sources (Fig. 4C, probe dh).

Clr6 is required for *per1* chromatin acetylation. The different levels of acetylated H4K12 for *per1* could be due to a change in deacetylation or acetylation, or both. To distinguish between these possibilities, we examined the H4K12 acetylation profile of *per1* in strains lacking *hat1* or carrying the *clr6-1* mutant allele. As shown in Fig. 5A, ChIP analysis of chromatin from *hat1*Δ cells showed a H4K12ac profile similar to that of wt cells, with higher levels of acetylation in ammonia than in proline (Fig. 5A, left). In contrast, *clr6-1* cells showed little difference in H4K12 acetylation between ammonia and proline (Fig. 5A, right). Especially over probes 5 and 6, which cover the middle and the 3′ end of the *per1* ORF, H4K12 acetylation was as high or even higher in *clr6-1* cells grown in proline than in those grown in ammonia. Note that the absolute levels of ChIP signal were lower in *clr6-1* than in the wt, as shown in Fig. 4B, likely due to differences in the genetic background. Furthermore, when grown in proline, the *clr6-1* mutant did not produce transcripts B and C (Fig. 5B, left and middle). In RNA isolated from a *hat1*Δ strain, however, transcripts B and C were detectable, as in wt cells (Fig. 5B, left and middle). These results suggest that Clr6, but not Hat1, is involved in deacetylation of H4K12 at the *per1* locus and in expression of transcript B. Consistently, *clr6-1* mutant cells displayed a growth defect with proline as the nitrogen source, whereas *hat1*Δ cells grew normally (Fig. 1B).

The constitutive expression of transcript B and the reduced levels of H4K12 acetylation that we observed in *oca2*Δ cells may therefore be due to increased Clr6 activity in the strain. To test this assumption, we examined *per1* expression and H4K12 acetylation in an *oca2*Δ strain also carrying the *clr6-1* allele. In contrast to *oca2*Δ, the *oca2*Δ *clr6-1* double mutant did not produce transcripts B and C when grown in ammonia, suggesting that Clr6 activity is responsible for their aberrant expression in *oca2*Δ (Fig. 5C, compare lanes 1 and 7 with lanes 3 and 9). Furthermore, H4K12 acetylation at *per1* was higher in *oca2*Δ *clr6-1* than in *oca2*Δ cells, indicating that reduced H4K12 acetylation in *oca2*Δ cells grown in ammonia is due to increased Clr6 activity (Fig. 5D, compare left and middle). This result indicates that Oca2 and Clr6 have opposing effects on *per1* expression, with Oca2 acting as a repressor and Clr6 as an activator. Furthermore, because *clr6-1* is epistatic to *oca2*Δ, this suggests that Oca2 controls Clr6 activity in ammonia. Consistent with this hypothesis, the *oca2*Δ *clr6-1* strain had a growth phenotype similar to that of *clr6-1*, with better growth in ammonia than in proline (Fig. 5E).

RNAi-mediated silencing factors are involved in *per1* repression. Oca2 also interacts with the RITS component Ago1 (Fig. 1D), which promotes silencing in heterochromatic regions, including centromeres (12). Moreover, *per1* is located adjacent to the left outermost centromeric repeat on chromosome 1 (Fig. 6A), and *ago1*Δ cells grow more slowly in ammonia than in proline, similar to *oca2*Δ cells (Fig. 1B). All of these observations suggest that Ago1 and the heterochromatic silencing machinery may be involved in regulation of *per1* expression. Furthermore, Northern blot analysis revealed that in cells lacking *ago1*, transcripts B and C are expressed under noninducing conditions, as in *oca2*Δ cells (Fig. 6B). Ago1 functions together with Dcr1, an RNase III enzyme, and with Clr4, a histone H3 lysine 9 methyltransferase, both involved in heterochromatic silencing (12). *clr4*Δ cells were therefore tested and shown by

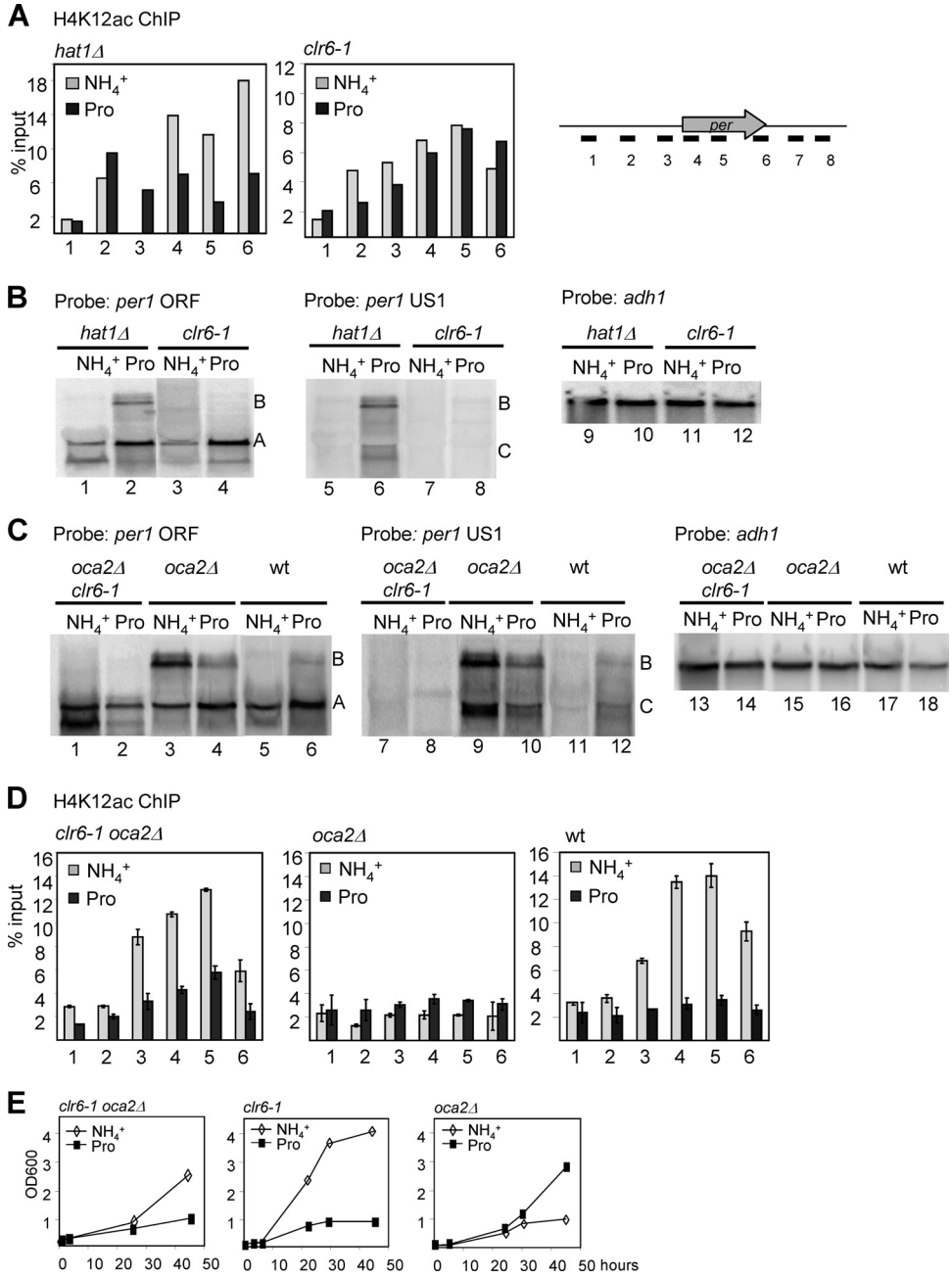

FIG. 5. Clr6 is required for the deacetylation of *per1* and for the accumulation of 5′-extended transcripts. (A) H4K12ac ChIP of *hat1*Δ and *clr6-1* cells grown in EMM containing either ammonia or proline. The positions of the PCR primers across the *per1* locus are indicated. (B) Northern blot analysis of total RNA isolated from *hat1*Δ and *clr6-1* cells grown in ammonia or proline, respectively. The probes were specific for the ORF of *per1* (left), the upstream region of *per1* (middle), and the ORF of *adh1* (right). (C) As for panel B, but using RNA isolated from *oca2*Δ *clr6-1*, *oca2*Δ, and wt cells. (D) H4K12ac ChIP analysis. *oca2*Δ *clr6-1*, *oca2*Δ, and wt cells were grown in either ammonia or proline, and H4K12ac distribution was analyzed using anti-H4K12ac antibody and *per1*-specific primer pairs as indicated. The error bars indicate SEM. (E) Growth phenotypes of *oca2*Δ *clr6-1*, *clr6-1*, and *oca2*Δ cells.

Northern blot analysis to exhibit an aberrant *per1* expression profile similar to that of *ago1*Δ and *oca2*Δ cells (Fig. 6B). Growth of *dcr1*Δ cells was too poor in these nitrogen sources to examine *per1* expression. Using a Flag-tagged *ago1* strain, we found that in the presence of ammonia, low levels of Ago1 localized to *per1* chromatin and that this association increased when the cells were grown in proline (Fig. 6C). Under these same conditions, more Ago1 also localized to the centromeric repeats (Fig. 6C, probe dh). Mutants in the heterochromatic silencing machinery lead to an accumulation of centromeric transcripts (14, 48). Using RT-PCR with primers specific for the centromeric dh repeats, we observed an increase of centromeric transcripts in *oca2*Δ cells (Fig. 6D). These results suggest that Ago1 and the heterochromatic silencing machin-

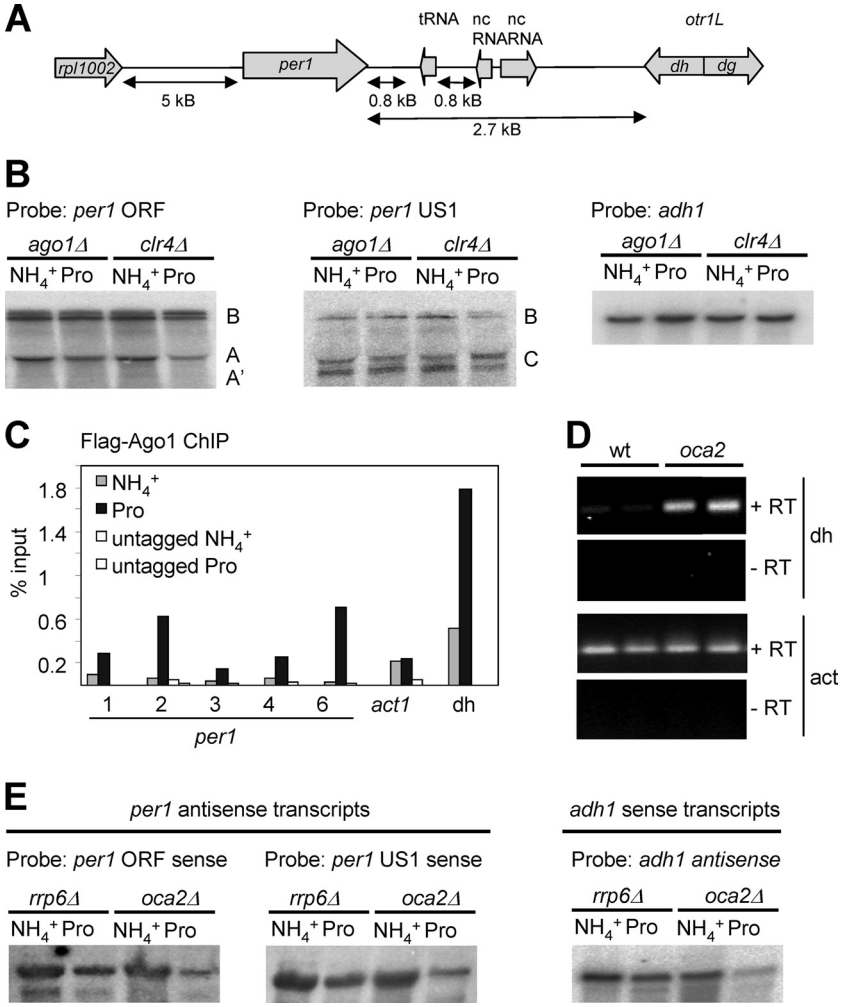

FIG. 6. Ago1 is involved in regulation of *per1*. (A) Schematic representation of the *per1* genomic region. nc, noncoding. (B) Northern blot analysis of *per1* mRNA from *ago1*Δ and *clr4*Δ cells using probes ORF (left), US1 (middle), and *adh1* (right). (C) ChIP analysis of Ago1 using a *Flag-ago1* strain and anti-Flag antibody. Primer probes 1, 2, 3, 4, and 6 were specific for *per1*, as indicated. Probes act1 and dh were specific for *act1* and the dh centromeric repeat, respectively. An untagged strain was used as a negative control. (D) RT-PCR of centromeric (dh) and actin transcripts using RNA isolated from wt and *oca2*Δ cells grown in ammonia. RNA was reverse transcribed using random hexamers and PCR amplified using primers specific for the dh centromeric repeat or actin. (E) Northern blot analysis of *per1* antisense transcripts from *rrp6*Δ and *oca2*Δ cells using single-stranded RNA probes mapping to the ORF (left) and US1 (middle) of *per1*. (Right) Loading control using a single-stranded RNA probe specific for sense *adh1* transcripts.

ery are involved in the regulation of *per1* and that the repression of *per1* and the centromeric repeats may be connected. However, using an antibody against dimethylated H3K9dime, a histone mark associated with silenced centromeric chromatin, we did not detect any significant changes in the levels or in the distribution of H3K9dime at *per1* in *oca2*Δ cells (data not shown), indicating that this histone modification is not involved in *per1* regulation. Given the involvement of RNAi factors in *per1* regulation, we also tested whether antisense transcription might play a role in *per1* regulation. Using sense RNA probes to the ORF and the upstream region of *per1*, we detected antisense *per1* transcripts in wt cells (not shown) and in *rrp6*Δ and *oca2*Δ cells (Fig. 6E). Absence of the exosome subunit Rrp6 did not lead to an accumulation of antisense transcripts (not shown). However, changing the nitrogen source from ammonia to proline or the absence of *oca2* did not correlate with a significant alteration in the levels or pattern of antisense transcripts, suggesting that regulation of *per1* does not employ an antisense or small interfering RNA (siRNA)-based mechanism.

DISCUSSION

We provide evidence for the transcriptional regulation of *per1* in response to the quality of the nitrogen source. We show that in the presence of ammonia, when *per1* expression is low, a transcript of about 2.8 kb is synthesized, and a region encompassing the coding and upstream regions of *per1* is acetylated. Transcriptional activation of *per1* by proline leads to transcription initiation from an additional upstream start site and correlates with deacetylation of the *per1* locus. Transcriptional activation and histone deacetylation of *per1* are constitutive in cells lacking the serine/threonine kinase gene *oca2* but

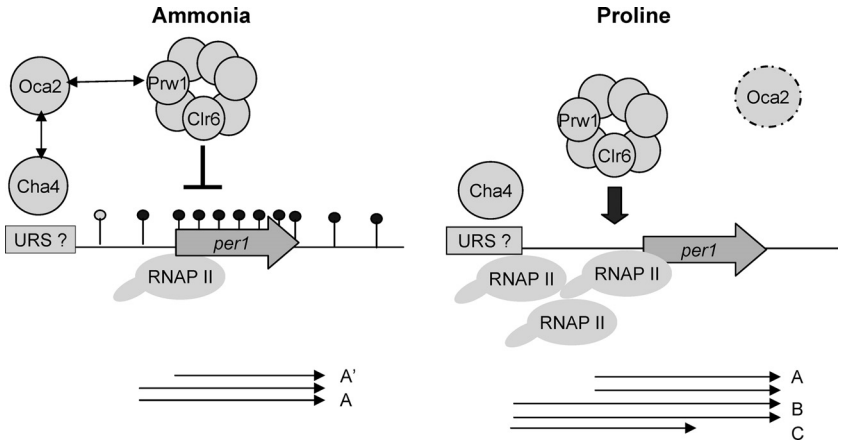

FIG. 7. Model for transcriptional regulation of *per1* by Oca2, Clr6, and Cha4. See the text for details. RNAP II, Pol II.

are reduced in *clr6-1* cells under inducing conditions, suggesting that Oca2 and Clr6 act in opposite directions as a repressor and activator, respectively, of *per1* expression. In an *oca2*Δ *clr6-1* double mutant, stimulation of *per1* and H4K12 deacetylation under noninducing conditions are no longer observed, suggesting that Clr6 acts downstream of Oca2 and that the phenotype of *oca2*Δ cells may be due to aberrant Clr6 activity. Oca2 interacts with the predicted transcriptional activator Cha4, as well as with Ago1, a factor involved in heterochromatin silencing. Cha4 appears to be required for both repression and activation of *per1*. As with *oca2*, loss of *ago1* leads to activation of *per1* under repressing conditions, suggesting that Ago1 acts as a repressor of the *per1* gene.

These observations can be tied together by the following model (Fig. 7). If ammonia is available, Oca2 represses Clr6 activity, possibly through interaction with Prw1. As a result, H4K12 actylation at *per1* is high, allowing only expression of transcript A. This may be sufficient to produce limited amounts of permease protein required for the import of amino acids for anabolic purposes. When cells are grown in proline, levels of Oca2 protein are reduced, analogous to the *oca2*Δ strain. As a result, Clr6 activity is no longer repressed, which leads to H4K12 deacetylation at *per1*, recruitment of Pol II to the upstream initiation site, and synthesis of 5′-extended transcripts. It may be that the longer *per1* mRNA 5′ UTR contains *cis*-acting signals that allow improved binding of the translation machinery and hence more efficient protein synthesis. Transcriptional induction by proline would therefore involve not only increased levels of *per1* transcription, but also the production of translationally more competent transcripts, ensuring that the cell produces enough permease protein for the efficient import of proline for catabolic use as a nitrogen source. In this model, Clr6 deacetylates *per1* and surrounding regions in a nontargeted way when cells use proline. Only when ammonia becomes available does the activity of Clr6 become locally restricted at *per1* through targeted recruitment of the repressor Oca2. Deacetylation and activation would thus be the default pathway for *per1* expression. This model is attractive, as in the natural habitat of *S. pombe*, proline is the most abundant nitrogen source (18).

Oca2 may be recruited to *per1* in ammonia via interaction with Cha4, which in turn binds to upstream regulatory sequences through its Zn finger domain. In the presence of proline, Cha4 may recruit a different, *per1*-activating protein. Cha4 would thus act as a corepressor of *per1* expression in ammonia but as a coactivator in proline, explaining the opposite phenotypes of the *cha4*Δ strain in the two nitrogen sources. A possible candidate for this *per1*-activating protein could be the SWI/SNF remodeling complex, as in *S. cerevisiae*, Cha4 recruits SWI/SNF as a coactivator of *SRG1* transcription (28). Preliminary evidence indicates that Snf22, a component of the SWI/SNF complex in *S. pombe*, may indeed be involved in activation of *per1*, as a *snf22*Δ mutant strain showed a reduction in upstream start site selection in proline (see Fig. S6 in the supplemental material). Ago1 may act as a repressor of *per1* expression under noninducing conditions (see below).

Role of histone deacetylation in gene activation. We found that *clr6-1* negatively affects *per1* expression, suggesting that Clr6 acts as an activator of *per1* transcription. This is in agreement with a previous report that investigated the global effects of *clr6-1* on gene expression (14). However, another genome-wide study found *per1* to be upregulated in *clr6-1* (52). A possible explanation for this discrepancy is that in the latter studies rich medium was employed for cell growth, which may trigger a different transcriptional response than minimal medium, used by Hansen et al. (14) and in this study.

Histone deacetylation has traditionally been associated with transcription repression. On a global level, this is true, as shown by genome-wide analysis of enzymatic activities and gene expression profiling (36, 52). However, several reports investigating specific genes have provided evidence that histone deacetylation can also activate transcription. In *S. cerevisiae*, Rpd3 has been shown to be directly required for transcriptional activation of osmoresponsive, DNA damage-inducible, and anaerobic genes (10, 43, 44). In response to the corresponding stimuli, Rpd3 is recruited to and deacetylates the promoters of these genes. Rpd3, together with the related HDAC Hos2, also plays a positive role in transcription of the *GAL* genes, but here, the coding regions are affected (49).

In this study, we found that histone deacetylation at *per1* correlated with transcriptional activation of *per1*, indicating an activating role of Clr6. Because *clr6-1* showed a defect in both

deacetylation and transcriptional activation, deacetylation of *per1* seems to be a cause for, and not an effect of, increased transcription. Importantly, deacetylation of *per1* leads not only to increased transcription, but also to the use of an upstream initiation site. Possibly, histone deacetylation of *per1* induces chromatin remodeling over upstream and coding regions, for instance, by SWI/SNF. This could make alternative initiation sites accessible, as well as promote more efficient Pol II elongation over coding regions.

Oca2 also interacts with the type B histone acetyltransferase Hat1; however, in a *hat1*Δ strain, we did not detect changes in H4K12 acetylation or a defect in *per1* expression. Perhaps Hat1 may be required for genes other than *per1*, for instance, genes that are located in the subtelomeric regions. Similarly, in *S. cerevisiae*, Hat1 has been implicated in telomeric silencing (23).

Gene regulation through upstream initiation. Gene regulation through the use of upstream transcription initiation sites has recently been reported for two other *S. pombe* genes, *tco1* and *fbp1* (16, 42). In the case of *fbp1*, glucose starvation-induced activation leads first to the synthesis of 5′-extended noncoding transcripts and only later to accumulation of the main, shorter *fbp1* transcript. This study showed that passage of Pol II through the *fbp1* upstream region is required for progressive conversion of the *fbp1* chromatin into an open configuration, allowing Pol II to initiate from the genuine downstream initiation site (16). In the case of *tco1*, low oxygen shifts transcription initiation to an upstream site, which leads to downregulation of *tco1*. The resulting longer transcript is translationally silent, as it fails to associate with polysomes, possibly due to formation of inhibitory secondary structures in its 5′ UTR (42). We do not know whether transcript B is translated differently from the shorter transcript A. However, as more Per1 protein is required when proline is used as a nitrogen source (46), it seems plausible that the longer mRNA is translationally more competent. The possibility that transcript B encodes a different protein is excluded, as its extended 5′ UTR does not possess a continuous reading frame (data not shown).

Connection between transcription initiation and termination. Oca2 was originally isolated as a multicopy suppressor of a transcription termination mutant (2; Azad and Proudfoot, unpublished). However, the role of Oca2 in transcription termination has remained elusive. It may be that Oca2 is involved in both transcription initiation and termination. A similar role in different stages of transcription was shown for the *S. cerevisiae* chromatin-remodeling proteins Chd1, Isw1, and Isw2. Depending on which gene they act on, these proteins can modulate the association of initiation factors with the promoter, the release of Pol II into productive elongation, or the pausing and release of the polymerase at the terminator (1, 32). However, it is also possible that complementation of the transcription termination mutant by overexpressing *oca2* was indirect. The screen that led to the isolation of *oca2* employed a modified *ura4* gene containing an intronic terminator and selected for clones that revert from uracil prototrophy to auxotrophy. Thus, it may be that complementation by overexpressed *oca2* was due to reduced expression of a transporter gene involved in uracil metabolism rather than restored *ura4* transcription termination.

Genome-wide function of Oca2. Expression of Oca2 is upregulated as part of the core environmental-stress response (8a), which suggests that Oca2 functions in a variety of stress response pathways, one of them possibly being changes in nutrient availability. Our whole-genome expression analysis found that loss of *oca2* leads to upregulation of genes encoding membrane transporter proteins that localize near telomeric regions. A previous report showed that nitrogen starvation-responsive genes are clustered in the subtelomeric regions (29). Thus, it appears that proline or loss of *oca2* triggers a transcriptional response related to nitrogen starvation. Importantly, the upregulated genes in *oca2*Δ cells overlap with genes downregulated in *clr6-1* mutants, notably, *per1* (14). This study also demonstrated that the upregulated genes in *oca2*Δ cells showed significant overlap with the genes induced in *clr1* and *clr3* mutants, silencing proteins that act redundantly with the RNAi pathway (14).

Interconnection of Oca2 with Cha4 and Ago1. We have demonstrated that Oca2 interacts with Cha4, a zinc finger protein, and with Ago1, a factor involved in RNAi-induced transcriptional silencing. Cha4 is related to the *S. cerevisiae* DNA-binding proteins Cha4 and Tea1; it is thus likely that in *S. pombe* Cha4 binds to regulatory DNA sequences as well. In *S. cerevisiae*, Cha4 has been shown to act as an activator of the serine-responsive gene *CHA1*, encoding a serine deaminase (17), and of the regulatory RNA *SRG1*, which in turn represses expression of the serine-biosynthetic gene *SER3* (28). This raises the possibility that *S. pombe* Cha4 may also act as a regulator of genes involved in amino acid metabolism. Interestingly, the *CHA1* promoter is located 2 kb downstream of the silent-mating-type locus *HML*, reminiscent of the proximity of *per1* to the centromeric region, and repression of *CHA1* under noninducing conditions requires Sir4, a factor involved in chromatin silencing in *S. cerevisiae* (30). In this study, we observed that Oca2 interacts with Ago1 and that *ago1*Δ and *clr4*Δ cells derepress *per1* under noninducing conditions. Also, Ago1 localizes to *per1*, suggesting that Ago1 and heterochromatic silencing may be involved in *per1* regulation. Since *per1* is located close to the left outermost centromeric repeat on chromosome 1 and *oca2*Δ cells display an accumulation of centromeric transcripts, it is possible that *per1* regulation may be controlled by a position effect due to its proximity to the centromere. Likewise, the other upregulated genes in *oca2*Δ may be controlled through their positions in the subtelomeric regions. Mutants in the *S. pombe* RNAi and the chromatin-silencing machineries have all been shown to affect expression of a large number of endogenous genes, including the *mat2-P* and *mat3-M* silent loci in the mating-type region and many genes that are clustered in the subtelomeric regions (14, 47). Likewise, heterologous genes placed within or adjacent to heterochromatic locations are subject to transcriptional repression (13, 48). However, neither H3K9me, the histone modification typically found in heterochromatic regions, nor antisense transcription appears to correlate with *per1* regulation. Therefore, *per1* regulation seems not to employ an siRNA-based silencing mechanism; instead, Ago1 and Clr4 may play alternative roles.

General connections of Oca2 with Tor and nutrient-dependent growth. Rapamycin binds to TOR, a universally conserved kinase that couples nutrient availability to cell growth. In budding yeast and higher eukaryotes, inhibition of TOR by

rapamycin triggers a variety of transcriptional and translational responses, similar to nutrient starvation. In fission yeast, inhibition of Tor by rapamycin leads to the reduced expression of amino acid permease genes, including *per1* and *put4* (50). It is possible that the positive effect of rapamycin on the growth of *oca2*Δ is due to downregulation of these genes in the presence of the drug. In *S. cerevisiae*, rapamycin affects transcription of target genes through changes in the recruitment of Rpd3 (19, 37). Moreover, in *S. pombe*, *tor1*Δ mutants show an overlapping gene expression pattern like *clr6-1* mutants (41), suggesting that Tor and Clr6 may act in the same pathway. It remains to be shown whether rapamycin affects recruitment of Clr6 and histone deactylation at *per1*.

Overall, our studies of *per1* indicate that *S. pombe* has evolved a sophisticated network of gene regulation through chromatin modification to control the expression of membrane transporter proteins and the consequent utilization of nitrogen.

ACKNOWLEDGMENTS

We thank Karl Ekwall, Robin Allshire, Marc Bühler, Danesh Moazed, Chris Norbury, Keith Gull, Fred Winston, and Stefania Castagnetti for strains and reagents. We also thank Jurgi Camblong for helpful discussions and comments on the manuscript.

This work was supported by Programme Grants from the Medical Research Council and the Wellcome Trust to N.J.P., and a Cancer Research United Kingdom grant to J.B. S.M. was supported by a Swiss National Science Foundation Advanced Researchers fellowship.

REFERENCES

1. **Alén, C., N. A. Kent, H. S. Jones, J. O'Sullivan, A. Aranda, and N. J. Proudfoot.** 2002. A role for chromatin remodeling in transcriptional termination by RNA polymerase II. Mol. Cell **10:**1441–1452.
2. **Aranda, A., and N. Proudfoot.** 2001. Transcriptional termination factors for RNA polymerase II in yeast. Mol. Cell **7:**1003–1011.
3. **Bähler, J., J. Q. Wu, M. S. Longtine, N. G. Shah, A. McKenzie III, A. B. Steever, A. Wach, P. Philippsen, and J. R. Pringle.** 1998. Heterologous modules for efficient and versatile PCR-based gene targeting in Schizosaccharomyces pombe. Yeast **14:**943–951.
4. **Benson, L. J., J. A. Phillips, Y. Gu, M. R. Parthun, C. S. Hoffman, and A. T. Annunziato.** 2007. Properties of the type B histone acetyltransferase Hat1:H4 tail interaction, site preference, and involvement in DNA repair. J. Biol. Chem. **282:**836–842.
5. **Bimbó, A., Y. Jia, S. L. Poh, R. K. Karuturi, N. den Elzen, X. Peng, L. Zheng, M. O'Connell, E. T. Liu, M. K. Balasubramanian, and J. Liu.** 2005. Systematic deletion analysis of fission yeast protein kinases. Eukaryot. Cell **4:**799–813.
6. **Buker, S. M., T. Iida, M. Bühler, J. Villén, S. P. Gygi, J.-I. Nakayama, and D. Moazed.** 2007. Two different Argonaute complexes are required for siRNA generation and heterochromatin assembly in fission yeast. Nat. Struct. Mol. Biol. **14:**200–207.
7. **Camblong, J., N. Iglesias, C. Fickentscher, G. Dieppois, and F. Stutz.** 2007. Antisense RNA stabilization induces transcriptional gene silencing via histone deacetylation in S. cerevisiae. Cell **131:**706–717.
8. **Carrozza, M. J., B. Li, L. Florens, T. Suganuma, S. K. Swanson, K. K. Lee, W. J. Shia, S. Anderson, J. Yates, M. P. Washburn, and J. L. Workman.** 2005. Histone H3 methylation by Set2 directs deacetylation of coding regions by Rpd3S to suppress spurious intragenic transcription. Cell **123:**581–592.

8a. **Chen, D., W. M. Toone, J. Mata, R. Lyne, G. Burns, K. Kivinen, A. Brazma, N. Jones, and J. Bahlar.** 2003. Global transcriptional responses of fission yeast to environmental stress. Mol. Biol. Cell **14:**214–219.

9. **De Craene, J. O., O. Soetens, and B. Andre.** 2001. The Npr1 kinase controls biosynthetic and endocytic sorting of the yeast Gap1 permease. J. Biol. Chem. **276:**43939–43948.
10. **De Nadal, E., M. Zapater, P. M. Alepuz, L. Sumoy, G. Mas, and F. Posas.** 2004. The MAPK Hog1 recruits Rpd3 histone deacetylase to activate osmoresponsive genes. Nature **427:**370–374.

10a. **Gray, W. M., and J. S. Fassler.** 1996. Isolation and analysis of the yeast *TEA1* gene, which encodes a zinc cluster Ty enhancer-binding protein. Mol. Cell. Bol. **16:**347–358.

11. **Grewal, S. I., M. J. Bonaduce, and A. J. Klar.** 1998. Histone deacetylase homologs regulate epigenetic inheritance of transcriptional silencing and chromosome segregation in fission yeast. Genetics **150:**563–576.
12. **Grewal, S. I., and S. Jia.** 2007. Heterochromatin revisited. Nat. Rev. Genet. **8:**35–46.
13. **Hall, I. M., G. D. Shankaranarayana, K. Noma, N. Ayoub, A. Cohen, and S. I. Grewal.** 2002. Establishment and maintenance of a heterochromatin domain. Science **297:**2232–2237.
14. **Hansen, K. R., G. Burns, J. Mata, T. A. Volpe, R. A. Martienssen, J. Bahler, and G. Thon.** 2005. Global effects on gene expression in fission yeast by silencing and RNA interference machineries. Mol. Cell. Biol. **25:**590–601.
15. **Hayashi, T., Y. Fujita, O. Iwasaki, Y. Adachi, K. Takahashi, and M. Yanagida.** 2004. Mis16 and Mis18 are required for CENP-A loading and histone deacetylation at centromeres. Cell **118:**715–729.
16. **Hirota, K., T. Miyoshi, K. Kugou, C. S. Hoffman, T. Shibata, and K. Ohta.** 2008. Stepwise chromatin remodelling by a cascade of transcription initiation of non-coding RNAs. Nature **456:**130–134.
17. **Holmberg, S., and P. Schjerling.** 1996. Cha4p of Saccharomyces cerevisiae activates transcription via serine/threonine response elements. Genetics **144:**467–478.
18. **Huang, H. L., and M. C. Brandriss.** 2000. The regulator of the yeast proline utilization pathway is differentially phosphorylated in response to the quality of the nitrogen source. Mol. Cell. Biol. **20:**892–899.
19. **Humphrey, E. L., A. F. Shamji, B. E. Bernstein, and S. L. Schreiber.** 2004. Rpd3p relocation mediates a transcriptional response to rapamycin in yeast. Chem. Biol. **11:**295–299.
20. **Hunter, T., and G. D. Plowman.** 1997. The protein kinases of budding yeast: six score and more. Trends Biochem. Sci. **22:**18–22.
21. **Irvine, D. V., M. Zaratiegui, N. H. Tolia, D. B. Goto, D. H. Chitwood, M. W. Vaughn, L. Joshua-Tor, and R. A. Martienssen.** 2006. Argonaute slicing is required for heterochromatic silencing and spreading. Science **313:**1134–1137.
22. **Johnston, S. D., S. Enomoto, L. Schneper, M. C. McClellan, F. Twu, N. D. Montgomery, S. A. Haney, J. R. Broach, and J. Berman.** 2001. CAC3(MSI1) suppression of RAS2(G19V) is independent of chromatin assembly factor I and mediated by NPR1. Mol. Cell. Biol. **21:**1784–1794.
23. **Kelly, T. J., S. Qin, D. E. Gottschling, and M. R. Parthun.** 2000. Type B histone acetyltransferase Hat1p participates in telomeric silencing. Mol. Cell. Biol. **20:**7051–7058.
24. **Keogh, M. C., S. K. Kurdistani, S. A. Morris, S. H. Ahn, V. Podolny, S. R. Collins, M. Schuldiner, K. Chin, T. Punna, N. J. Thompson, C. Boone, A. Emili, J. S. Weissman, T. R. Hughes, B. D. Strahl, M. Grunstein, J. F. Greenblatt, S. Buratowski, and N. J. Krogan.** 2005. Cotranscriptional set2 methylation of histone H3 lysine 36 recruits a repressive Rpd3 complex. Cell **123:**593–605.
25. **Kurdistani, S. K., and M. Grunstein.** 2003. Histone acetylation and deacetylation in yeast. Nat. Rev. Mol. Cell Biol. **4:**276–284.
26. **Kurdistani, S. K., D. Robyr, S. Tavazoie, and M. Grunstein.** 2002. Genome-wide binding map of the histone deacetylase Rpd3 in yeast. Nat. Genet. **31:**248–254.
27. **Lyne, R., G. Burns, J. Mata, C. J. Penkett, G. Rustici, D. Chen, C. Langford, D. Vetrie, and J. Bahler.** 2003. Whole-genome microarrays of fission yeast: characteristics, accuracy, reproducibility, and processing of array data. BMC Genomics **4:**27.
28. **Martens, J. A., P. Y. Wu, and F. Winston.** 2005. Regulation of an intergenic transcript controls adjacent gene transcription in Saccharomyces cerevisiae. Genes Dev. **19:**2695–2704.
29. **Mata, J., R. Lyne, G. Burns, and J. Bahler.** 2002. The transcriptional program of meiosis and sporulation in fission yeast. Nat. Genet. **32:**143–147.
30. **Moreira, J. M., and S. Holmberg.** 1998. Nucleosome structure of the yeast CHA1 promoter: analysis of activation-dependent chromatin remodeling of an RNA-polymerase-II-transcribed gene in TBP and RNA pol II mutants defective in vivo in response to acidic activators. EMBO J. **17:**6028–6038.
31. **Moreno, S., A. Klar, and P. Nurse.** 1991. Molecular genetic analysis of fission yeast Schizosaccharomyces pombe. Methods Enzymol. **194:**795–823.
32. **Morillon, A., N. Karabetsou, J. O'Sullivan, N. Kent, N. Proudfoot, and J. Mellor.** 2003. Isw1 chromatin remodeling ATPase coordinates transcription elongation and termination by RNA polymerase II. Cell **115:**425–435.
33. **Nicolas, E., T. Yamada, H. P. Cam, P. C. Fitzgerald, R. Kobayashi, and S. I. Grewal.** 2007. Distinct roles of HDAC complexes in promoter silencing, antisense suppression and DNA damage protection. Nat. Struct. Mol. Biol. **14:**372–380.
34. **Parthun, M. R.** 2007. Hat1: the emerging cellular roles of a type B histone acetyltransferase. Oncogene **26:**5319–5328.
35. **Pidoux, A., B. Mellone, and R. Allshire.** 2004. Analysis of chromatin in fission yeast. Methods **33:**252–259.
36. **Robyr, D., Y. Suka, I. Xenarios, S. K. Kurdistani, A. Wang, N. Suka, and M. Grunstein.** 2002. Microarray deacetylation maps determine genome-wide functions for yeast histone deacetylases. Cell **109:**437–446.
37. **Rohde, J. R., and M. E. Cardenas.** 2003. The TOR pathway regulates gene expression by linking nutrient sensing to histone acetylation. Mol. Cell. Biol. **23:**629–635.
38. **Rundlett, S. E., A. A. Carmen, R. Kobayashi, S. Bavykin, B. M. Turner, and M. Grunstein.** 1996. HDA1 and RPD3 are members of distinct yeast histone deacetylase complexes that regulate silencing and transcription. Proc. Natl. Acad. Sci. U. S. A. **93:**14503–14508.

39. **Schmid, M., and T. H. Jensen.** 2008. The exosome: a multipurpose RNA-decay machine. Trends Biochem. Sci. **33:**501–510.
40. **Schmidt, A., T. Beck, A. Koller, J. Kunz, and M. N. Hall.** 1998. The TOR nutrient signalling pathway phosphorylates NPR1 and inhibits turnover of the tryptophan permease. EMBO J. **17:**6924–6931.
41. **Schonbrun, M., D. Laor, L. Lopez-Maury, J. Bahler, M. Kupiec, and R. Weisman.** 2009. TOR complex 2 controls gene silencing, telomere length maintenance, and survival under DNA-damaging conditions. Mol. Cell. Biol. **29:**4584–4594.
42. **Sehgal, A., B. T. Hughes, and P. J. Espenshade.** 2008. Oxygen-dependent, alternative promoter controls translation of tco1+ in fission yeast. Nucleic Acids Res. **36:**2024–2031.
43. **Sertil, O., A. Vemula, S. L. Salmon, R. H. Morse, and C. V. Lowry.** 2007. Direct role for the Rpd3 complex in transcriptional induction of the anaerobic DAN/TIR genes in yeast. Mol. Cell. Biol. **27:**2037–2047.
44. **Sharma, V. M., R. S. Tomar, A. E. Dempsey, and J. C. Reese.** 2007. Histone deacetylases RPD3 and HOS2 regulate the transcriptional activation of DNA damage-inducible genes. Mol. Cell. Biol. **27:**3199–3210.
45. **Tallada, V. A., R. R. Daga, C. Palomeque, A. Garzon, and J. Jimenez.** 2002. Genome-wide search of Schizosaccharomyces pombe genes causing overexpression-mediated cell cycle defects. Yeast **19:**1139–1151.
46. **ter Schure, E. G., N. A. van Riel, and C. T. Verrips.** 2000. The role of ammonia metabolism in nitrogen catabolite repression in Saccharomyces cerevisiae. FEMS Microbiol. Rev. **24:**67–83.
47. **Thon, G., and A. J. Klar.** 1992. The clr1 locus regulates the expression of the cryptic mating-type loci of fission yeast. Genetics **131:**287–296.
48. **Volpe, T. A., C. Kidner, I. M. Hall, G. Teng, S. I. Grewal, and R. A. Martienssen.** 2002. Regulation of heterochromatic silencing and histone H3 lysine-9 methylation by RNAi. Science **297:**1833–1837.
49. **Wang, A., S. K. Kurdistani, and M. Grunstein.** 2002. Requirement of Hos2 histone deacetylase for gene activity in yeast. Science **298:**1412–1414.
50. **Weisman, R., I. Roitburg, T. Nahari, and M. Kupiec.** 2005. Regulation of leucine uptake by tor1+ in Schizosaccharomyces pombe is sensitive to rapamycin. Genetics **169:**539–550.
51. **Win, T. Z., A. L. Stevenson, and S. W. Wang.** 2006. Fission yeast Cid12 has dual functions in chromosome segregation and checkpoint control. Mol. Cell. Biol. **26:**4435–4447.
52. **Wirén, M., R. A. Silverstein, I. Sinha, J. Walfridsson, H. M. Lee, P. Laurenson, L. Pillus, D. Robyr, M. Grunstein, and K. Ekwall.** 2005. Genome-wide analysis of nucleosome density histone acetylation and HDAC function in fission yeast. EMBO J. **24:**2906–2918.